SOFT-DECISION DECODING WITH CELL TO CELL INTERFERENCE REMOVED SIGNAL IN NAND FLASH MEMORY

Dong-hwan Lee and Wonyong Sung

Department of Electrical Engineering and Computer Science, Seoul National University
Gwanak-gu, Seoul 151-744 Korea
Email: ldh@dsp.snu.ac.kr, wysung@snu.ac.kr

ABSTRACT

As the semiconductor feature size continuously decreases, the signal integrity of MLC (multi-level cell) NAND flash memory becomes degraded, which causes increased bit error rate and short retention time limit. Since it is well known that cell-to-cell interference (CCI) is one of the major sources of bit errors, several signal processing solutions to mitigate or remove the CCI have been developed. Even though these works show BER (bit error rate) performance improvement with hard-decision error correction, combining an interference canceller and soft-decision decoding still needs to be studied. In this research, we derive a mathematical formulation for computing the likelihood function of the CCI removed signal, and then propose a conditional LLR (log-likelihood ratio) to represent soft-reliability information for soft-decision error correction. The proposed soft-information computation scheme is applied to simulated NAND flash memory, and it is demonstrated that soft-decision error correction with the CCI removed signal significantly increases the retention time limit of MLC NAND flash memory.

Index Terms— Cell-to-cell interference, NAND flash memory, soft-information, error correcting code (ECC)

1. INTRODUCTION

The capacity of NAND flash memory has been increased continuously during the last decade, and as a result, NAND flash memory devices are used for diverse applications from mobile devices to SSDs (solid state drives). However, it is quite challenging to further increase the memory density partly due to the degraded signal reliability when the feature size is extremely small. Among various noise sources, the capacitance coupling effect or cell-to-cell interference (CCI) becomes the dominant source of bit errors for sub-20 nm NAND flash memory. According to [1], the amount of CCI becomes 50 % of the total noise when the pitch size is 20 nm. Therefore, removing the CCI becomes very critical for future generation of high density NAND flash memory.

There have been several works to develop signal processing solutions for the CCI cancellation. In [2], data post-compensation and pre-distortion techniques were proposed. Also, in [3], an adaptive LMS (least mean square) filter based coupling canceller was studied. Even though these techniques offer promising solutions for the CCI cancellation, they require unquantized threshold voltage signals as input, which is not practical when high speed memory access is needed. Recently, we proposed a least squares based CCI canceller (LS-CCIC) that shows satisfactory bit error correcting performance even with a small number of voltage sensing operations [4]. These previous works mainly focused on developing efficient CCI cancellation algorithms, but soft-decision error correction with the CCI removed signal still needs to be studied.

In this work, we propose a soft-information computation scheme to utilize the CCI removed signal for soft-decision error correction in NAND flash memory. Since the probability density function (PDF) of the CCI removed signal is quite different from that of the original threshold voltage, we derive a mathematical formulation for computing the likelihood function of the CCI removed signal, and then propose a soft-information computation scheme. The proposed method is applied to simulated NAND flash memory, and the BER (bit error rate) performance of a message passing decoder is evaluated.

This paper is organized as follows. Section 2 explains the signal modeling in 2-bit MLC (multi-level cell) NAND flash memory and, also, the CCI canceller. In Section 3, we derive the likelihood function of the CCI removed signal and propose a method for computing the conditional LLRs (log-likelihood ratios) for soft-decision error correction. In Section 4, experimental results are shown. Finally, concluding remarks are made in Section 5.

2. BACKGROUND

In this section, we explain the signal modeling of 2-bit MLC NAND flash memory as well as CCI cancellers that were previously proposed in [3, 4].

2.1. Signal modeling of 2-bit MLC NAND flash memory

The output signal obtained from 2-bit MLC NAND flash memory is frequently modeled as shown in Fig. 1. Multi-page programming is widely used in MLC NAND flash memory to reduce the amount of CCI while achieving a high write throughput [5]. In this programming scheme, LSB (least significant bit) and MSB (most significant bit) pages are programmed sequentially as shown in Fig. 2. After the LSB page programming, the CCI induced by programming of the neighboring cells is added to the threshold voltage of the victim cell, and the resulting voltage becomes V_L. In this paper, the mean of V_L is denoted as either m_1 or m_0 depending on the LSB value of a cell as shown in Fig. 2. When the MSB page programming is conducted, the threshold voltage becomes V_M. Because of the incremental stair pulse programming (ISPP), which results in an uniform threshold voltage distribution with the width of ΔV_{pp}, a tight threshold voltage bound can be achieved as shown in Fig. 2.

This work was supported by the Brain Korea 21 Project and the National Research Foundation of Korea (NRF) grants funded by the Ministry of Education, Science and Technology (MEST), Republic of Korea (No. 2012R1A2A2A06047297). Dong-hwan Lee was also financially supported by the NRF of Korea under the Global Ph.D. Fellowship project.

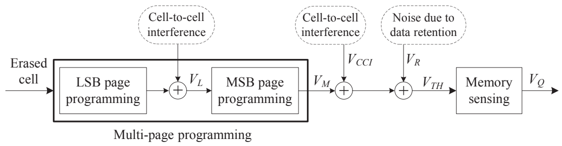

Fig. 1. Signal modeling for 2-bit MLC NAND flash memory.

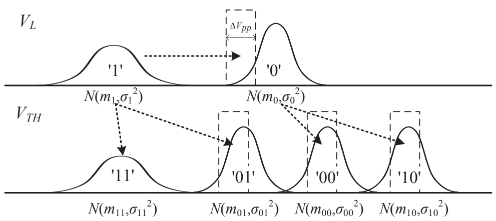

Fig. 2. Threshold voltage distribution of 2-bit MLC NAND flash memory.

The cell-to-cell interference is caused by the parasitic capacitor coupling effect among the adjacent cells. Thus, when one cell is programmed, the threshold voltages of both the target and the surrounding cells increase [6]. The amount of interference that the victim cell receives, V_{CCI}, can be represented as a linear combination of the threshold voltage shifts of the neighboring cells. In addition, the data retention problem, which is caused by the charge loss at the floating-gate, induces a negative shift of the threshold voltage, V_R. Thus, the threshold voltage of one cell becomes

$$V_{TH} = V_M + V_{CCI} + V_R. \tag{1}$$

According to [7], the PDF (probability density function) of V_{TH} can be modeled as a Gaussian mixture, and its mean and standard deviation values can be found by parametric estimation methods. In this paper, we denote the mean and standard deviation of the input symbol k as m_k and σ_k, respectively, for k = *11*, *01*, *00*, and *10* as shown in Fig. 2. After memory sensing operations, V_Q that includes the quantization effect on the threshold voltage signal is observed.

2.2. Cell-to-cell interference cancellation

The CCI canceller removes the correlation among the cells by employing signal processing algorithms that are similar to the adaptive equalization [2, 3, 4]. According to [4], the amount of interference can be estimated as follows:

$$V_{CCI} = \sum_{i=0}^{M-1} C_i \cdot \Delta V[i]. \tag{2}$$

In Eq. (2), $\Delta V[i]$ denotes the observed threshold voltage shift of the i-th neighbor cell. Note that M represents the number of interferencing cells and is either 3 (for odd victim cells) or 5 (for even victim cells) [6]. The CCI canceller coefficients are denoted as C_i, and finding the optimal values of them is very important to achieve a satisfactory BER performance. In [3], the adaptive LMS (least mean square) filtering is used to obtain C_i, while a least squares based approach is employed in [4]. Once the amount of CCI is estimated by using Eq. (2), it needs to be subtracted from the quantized memory sensing output signal V_Q. As a result, the CCI removed signal

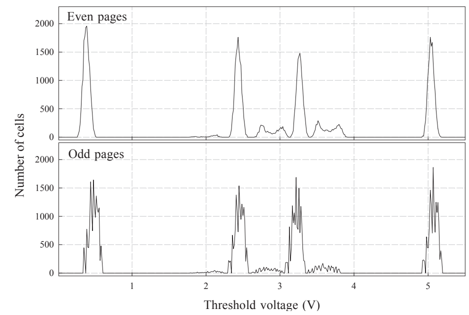

Fig. 3. Distribution of the CCI removed threshold voltage signals.

becomes

$$V_O = V_Q - V_{CCI}. \tag{3}$$

The optimal memory sensing schemes for the CCI canceller vary depending on the location of the sensed cells [4]. For victim cells, the MMI (maximum mutual information) quantization scheme that employs non-uniform quantization steps is suitable [8]. On the other hand, it was demonstrated that only a 4-level uniform quantizer (i.e. similar to normal hard-decision sensing) is enough for the surrounding cells to ensure satisfactory error correction performance of the CCI canceller [4].

3. SOFT-DECISION ERROR CORRECTION WITH CCI REMOVED SIGNAL

Accurate assessment of soft-information is important for soft-decision decoding to obtain the best error correcting performance. When the CCI cancellation is not applied, the likelihood function of the threshold voltage signal can be approximated to a Gaussian function, and hence computing LLR (log-likelihood ratio) is straightforward [9]. However, the distribution of the CCI removed signal is quite different from the original one as depicted in Fig. 3. In this section, we estimate the likelihood function of the CCI removed signal V_O and propose a soft-information computation scheme for reliable soft-decision error correction.

3.1. Estimation of CCI removed signal distribution

In order to estimate the likelihood function of the CCI removed signal, we need to derive those of V_{CCI} and V_Q. Let us denote the likelihood functions of V_{CCI} and V_Q as $f_{V_{CCI}|X}(v|k)$ and $f_{V_Q|X}(v|k)$, respectively. Note that X represents the input symbol and k corresponds to *11*, *01*, *00*, or *10*.

As explained in Section 2, V_{CCI} can be modeled as a linear combination of $\Delta V[i]$ that is *i.i.d* (independent and identically distributed). Thus, we can derive the mathematical formulation for the PDF of V_{CCI} by using that of $\Delta V[i]$. As shown in Fig. 1, $\Delta V[i]$ is equal to $V_{TH}[i] - V_L[i]$, and the PDFs of V_{TH} and V_L can be approximated to Gaussian mixtures according to [7]. As a result, $f_{\Delta V}(v)$ can also be represented as a Gaussian mixture as follows:

$$f_{\Delta V}(v) = \sum_k P_k \cdot N(m_k - m_{k_L}, \sigma_k^2 + \sigma_{k_L}^2), \tag{4}$$

where k_L and P_k denote the LSB symbol and the probability of the input symbol k, respectively. Note that $N(m, \sigma^2)$ represents a Gaussian distribution whose mean and variance are m and σ^2, respectively. By using Eq. (4), the mean and the variance of V_{CCI} can be

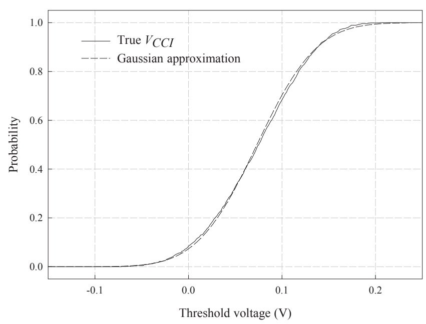

Fig. 4. Cumulative density functions of V_{CCI} and its Gaussian approximation.

computed quite simply as follows:

$$E[V_{CCI}] = m_{V_{CCI}} = \sum_{i=0}^{M-1} C_i \cdot E\Big[\Delta V[i]\Big] \tag{5}$$

and

$$Var[V_{CCI}] = \sigma^2_{V_{CCI}} = \sum_{i=0}^{M-1} C_i^2 \cdot Var\Big[\Delta V[i]\Big]. \tag{6}$$

Since V_{CCI} is independent from the input symbol of the victim cell k, $f_{V_{CCI}|X}(v|k)$ becomes $N(m_{V_{CCI}}, \sigma^2_{V_{CCI}})$. Figure 4 shows the CDFs (cumulative density functions) of V_{CCI} and its Gaussian approximation, and we can find that they are quite similar.

Next, let us find the likelihood function of V_Q. Recall that V_Q is the output of memory sensing applied to the victim cell. If we assume that an N_q-level MMI quantizer is used for memory sensing (e.g. Fig. 5 shows a 7-level MMI quantizer), the voltage region is divided into N_q levels and the likelihood function of V_Q becomes

$$f_{V_Q|X}(v|k) = \sum_{j=0}^{N_q-1} P_{k,j} \cdot \delta(v - r_j), \tag{7}$$

where r_j denotes the representative value of the voltage region $(q_j, q_{j+1}]$. Note that $P_{k,j}$ is the probability that the input symbol k falls into the voltage region j and $\delta(x)$ is the delta function.

If V_{CCI} and V_Q are independent each other, the likelihood function of V_O is the convolution of $f_{V_Q|X}(v|k)$ and $f_{V_{CCI}|X}(-v|k)$ according to Eq. (3). In reality, however, V_{CCI} and V_Q are not independent. Let us assume that 7-level voltage sensing is applied as shown in Fig. 5. If a cell whose input symbol is *01* has a threshold voltage at the region 3, it is highly likely that the cell has received quite large CCI. On the other hand, if one cell has an input symbol *00* and is observed at the same voltage region, the amount of CCI is probably small.

In order to compensate the correlation between V_{CCI} and V_Q, we modify the likelihood function of V_Q as follows:

$$f_{V_Q|X}(v|k) = \sum_{j=0}^{N_q-1} P_{k,j} \cdot \delta(v - r_{k,j}), \tag{8}$$

where

$$r_{k,j} = \begin{cases} G_k(q_{j-1}, q_j) & \text{if } (q_{j-1}, q_j] \text{ is an erasure region,} \\ r_j & \text{otherwise.} \end{cases} \tag{9}$$

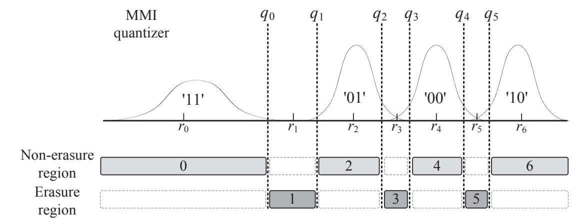

Fig. 5. 7-level MMI (maximum mutual information) quantization scheme.

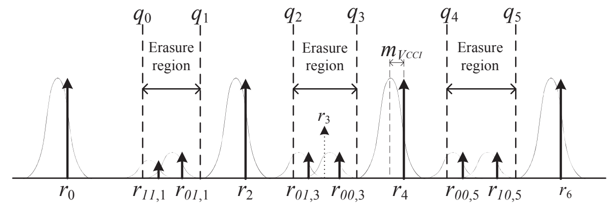

Fig. 6. Estimated distribution of the CCI removed signals.

In Eq. (9), $G_k(q_{j-1}, q_j)$ represents the center of mass or centroid of the region $(q_{j-1}, q_j]$ and can be computed as

$$G_k(q_{j-1}, q_j) = \frac{\int_{q_{j-1}}^{q_j} v f_{V_{TH}|X}(v|k)dv}{\int_{q_{j-1}}^{q_j} f_{V_{TH}|X}(v|k)dv}. \tag{10}$$

In the modified likelihood function of V_Q, the representative value of the erasure region is divided into two distinct ones depending on the input symbol. For example, r_3 (dotted arrow in Fig. 6) is divided into $r_{01,3}$ and $r_{00,3}$ (solid arrows in Fig. 6). By subtracting V_{CCI} from $r_{01,3}$ ($r_{00,3}$) rather than r_3, we can compensate the effect of large (small) CCI on the cells that have input symbols of *01* (*00*) and are observed at the voltage region 3.

By using $f_{V_Q|X}(v|k)$, $f_{V_{CCI}|X}(v|k)$, and Eq. (3), we can obtain the likelihood function of V_O as follows:

$$f_{V_O|X}(v|k) = f_{V_Q|X}(v|k) \bigotimes f_{V_{CCI}|X}(-v|k). \tag{11}$$

Note that $\bigotimes$ denotes the convolution operation. Figure 6 shows the threshold voltage distribution after the convolution.

3.2. Soft-information computation

By using the likelihood function of the CCI removed signal, we can define soft-information for LSB and MSB pages as follows:

$$\Lambda_L(v) = \begin{cases} \Lambda_{MAX} & \text{if } v < r_2 - m_{V_{CCI}}, \\ \ln \frac{f_{V_O|X}(v|01)}{f_{V_O|X}(v|00)} & \text{if } r_2 - m_{V_{CCI}} \le v < r_4 - m_{V_{CCI}}, \\ -\Lambda_{MAX} & \text{if } r_4 - m_{V_{CCI}} \le v, \end{cases} \tag{12}$$

and

$$\Lambda_M(v) = \begin{cases} \Lambda_{MAX} & \text{if } v < r_0 - m_{V_{CCI}}, \\ \ln \frac{f_{V_O|X}(v|11)}{f_{V_O|X}(v|01)} & \text{if } r_0 - m_{V_{CCI}} \leq v < r_2 - m_{V_{CCI}}, \\ -\Lambda_{MAX} & \text{if } r_2 - m_{V_{CCI}} \leq v < r_4 - m_{V_{CCI}}, \\ \ln \frac{f_{V_O|X}(v|10)}{f_{V_O|X}(v|00)} & \text{if } r_4 - m_{V_{CCI}} \leq v < r_6 - m_{V_{CCI}}, \\ \Lambda_{MAX} & \text{if } r_6 - m_{V_{CCI}} \leq v, \end{cases} \tag{13}$$

where Λ_{MAX} is a large positive constant. In order to reduce the computational overheads and offer more reliable soft-information, the LLR is set to Λ_{MAX} or $-\Lambda_{MAX}$ when the ECC decoding output is quite obvious. Equations (12) and (13) are for the case when 7-level voltage sensing is applied to the victim cells, and these equations can be modified quite easily when more voltage sensing operations are applied.

4. EXPERIMENTAL RESULTS

We conducted experiments to evaluate the post-ECC BER performance of the proposed soft-information computation scheme. During the experiments, the data samples obtained from the simulated 2-bit MLC NAND flash memory model [10] were used. Each block of the hypothetical NAND flash memory has 128 K bit-lines and 64 word-lines with the even/odd bit-line structure.

The post-ECC error performance of a (68254, 65536) EG-LDPC (Euclidean geometry low-density parity check) code [9] with the min-sum decoding algorithm was measured while changing the retention time. Also, we employed the least squares based CCI canceller (LS-CCIC) for CCI removal [4]. The 7-, 10-, and 13-level MMI quantizers are employed for the victim cells, while the 4-level uniform quantizer is used for the surrounding cells. For the comparison purpose, the error performances of soft-decision decoding without applying LS-CCIC are also presented. Note that 7-, 10-, and 13-level MMI quantizers demand 6, 9, and 12 sensing operations, respectively, while the 4-level uniform quantizer needs 3 sensing operations for each cell. To remove the CCI for the even victim cells, the five neighboring cells need to be read additionally, which demands 9 voltage sensing operations. For the odd victim cells, the three neighboring cells need to be read, and thus 6 more sensing operations are required.

Figure 7 shows the error performance of even MSB pages. Since the BER performance of LSB pages is quite similar to that of MSB pages except that all the curves are shifted to the right (higher retention time), we do not present it here. From Fig. 7, we can find that the BER performance is substantially improved by using the proposed soft-information computation scheme. The error performance of the LS-CCIC with 13-level quantization ('LS-CCIC, 13-level' in Fig. 7) is significantly improved when compared to the 'LDPC, unquantized' case that does not employ the LS-CCIC. Even for the 'LS-CCIC, 7-level' case, which demands 15 voltage sensing operations, its tolerable retention time is about three times longer than that of the 'LDPC, 16-level' case that requires the same number of voltage sensing operations.

Figure 8 shows the error performance for odd MSB pages. We can find that applying soft-decision error correction slightly improves the error performance even when the LS-CCIC is employed. The odd pages are less severely affected by the CCI than the even ones, thus removing the CCI does not guarantee a large improvement on the error performance. However, the retention time limits of odd pages are much longer than those of even pages. Thus, improving

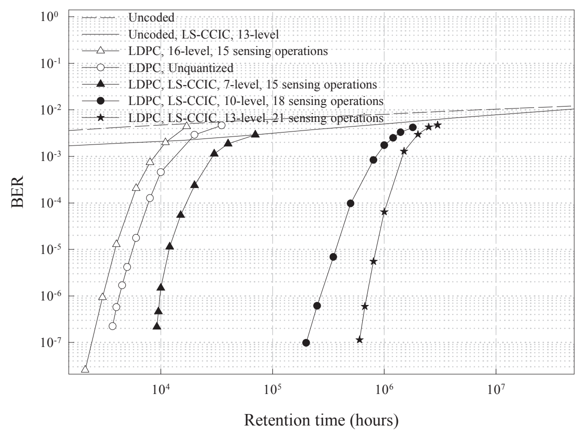

Fig. 7. Error performance of a (68254,65536) EG-LDPC code for even MSB pages.

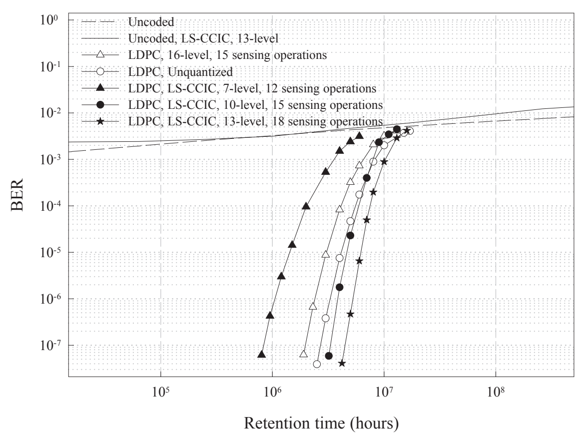

Fig. 8. Error performance of a (68254,65536) EG-LDPC code for odd MSB pages.

the BER performances of even pages is more important to increase the overall retention time limit of NAND flash memory.

5. CONCLUDING REMARKS

We have developed a soft-information computation method in order to combine the CCI cancellation algorithms and soft-decision error correction in MLC (multi-level cell) NAND flash memory. We derived a mathematical formulation for the likelihood function of the CCI removed signal and used it for soft-information computation. The developed algorithm is evaluated by using a simulated NAND flash memory model, and we obtain significant improvement on the worst case (even pages) post-ECC BER performance even when only a limited number of voltage sensing operations are used.

6. REFERENCES

[1] K. Prall, "Scaling non-volatile memory below 30nm," in *Proceedings of 22nd IEEE Non-Volatile Semiconductor Memory*

Workshop, 2007, pp. 5–10.

[2] G. Dong, S. Li, and T. Zhang, "Using data postcompensation and predistortion to tolerate cell-to-cell interference in MLC NAND flash memory," *IEEE Transactions on Circuits and Systems I: Regular Papers*, vol. 57, no. 10, pp. 2718–2728, 2010.

[3] D. Park and J. Lee, "Floating-gate coupling canceller for multi-level cell NAND flash," *IEEE Transactions on Magnetics*, vol. 47, no. 3, pp. 624–628, 2011.

[4] D. Lee and W. Sung, "Least squares based coupling cancelation for MLC NAND flash memory with a small number of voltage sensing operations," *Journal of Signal Processing Systems*, pp. 1–12, Dec. 2012.

[5] K.T. Park, M. Kang, D. Kim, S.W. Hwang, B.Y. Choi, Y.T. Lee, C. Kim, and K. Kim, "A zeroing cell-to-cell interference page architecture with temporary LSB storing and parallel MSB program scheme for MLC NAND flash memories," *IEEE Journal of Solid-State Circuits*, vol. 43, no. 4, pp. 919–928, 2008.

[6] J.D. Lee, S.H. Hur, and J.D. Choi, "Effects of floating-gate interference on NAND flash memory cell operation," *IEEE Electron Device Letters*, vol. 23, no. 5, pp. 264–266, 2002.

[7] D. Lee and W. Sung, "Estimation of NAND flash memory threshold voltage distribution for optimum soft-decision error correction," *IEEE Transactions on Signal Processing*, vol. 61, no. 2, pp. 440–449, Jan. 2013.

[8] J. Wang, T. Courtade, H. Shankar, and R. Wesel, "Soft information for LDPC decoding in flash: Mutual-information optimized quantization," in *Proceedings of IEEE Global Communications Conference (GLOBECOM)*, 2011, pp. 5–9.

[9] J. Kim, D. Lee, and W. Sung, "Performance of rate 0.96 (68254, 65536) EG-LDPC code for NAND flash memory error correction," in *Proceedings of IEEE International Conferences on Communications (ICC) Workshop on Emerging Data Storage Technologies*, 2012.

[10] G. Dong, Y. Pan, N. Xie, C. Varanasi, and T. Zhang, "Estimating information-theoretical NAND flash memory storage capacity and its implication to memory system design space exploration," *IEEE Transactions on Very Large Scale Integration (VLSI) Systems*, vol. 20, no. 9, pp. 1705–1714, 2012.